(d, $J = 5.9$, 3 H), 2.35 (s, 3 H), 3.65–3.58 (m, 6 H), 4.47–4.44 (dq, $J_1 = 5.99$, $J_2 = 2.12$, 1 H), 4.47 (s, 1 H), 7.18–7.16 (d, $J = 7.93$, 2 H), 7.77–7.75 (d, $J = 8.10$, 2 H), 8.58 (b, 1 H); IR (TF) 1770, 1500, 1440, 1250 cm^{-1}; FAB (cation) 185 (M$^+$), 142 (M$^+$ − 43).

3-(3-Bromo-4-methyl-2-oxoazetidinyl)-2-butenamide (32). To a solution of **21a** (94 mg, 0.369 mmol) and tetrabutylammonium bromide (237.5 mg, 0.738 mmol) in acetonitrile (1.5 mL) was added Et_3N (0.05 mL, 0.369 mmol). The reaction mixture was left for 44 h at room temperature and concentrated. The residue was poured into water (2 mL) and extracted with ethyl acetate (3 × 2 mL). The organic layers were combined, dried, and concentrated. The residue was purified by column chromatography with ethyl acetate–hexanes 1:2 to provide **32** (19 mg, 22%) and **22c** (13 mg, 22%) as oily compounds. Compound **32**: ^{1}H NMR δ 1.58–1.60 (d, $J = 6.30$, 3 H), 2.01 (s, 3 H), 4.14–4.30 (dq, $J_1 = 2.34$, $J_2 = 6.24$, 1 H), 4.30–4.31 (t, $J = 2.36$, 1 H), 5.03 (b, 1 H), 5.49 (s, 1 H), 8.76 (b, 1 H); IR (TF) 3420, 3305, 2980, 1775, 1630, 1540, 1310, 1235, 830 cm^{-1}; ^{13}C NMR δ 18.17, 46.68, 58.20, 86.63, 146.33, 161.12, 163.64; MS 248 (M$^+$ + 2), 246 (M$^+$), 155, 126, 84 (base peak). HRMS Calcd for $C_8H_{11}N_2O_2Br$: 246.00039. Found: 246.0001.

3-[3-[[2-(Trimethylsilyl)ethoxy]carbonyl]propyl]-3-[3-chloro-4-[3-[[2-(trimethylsilyl)ethoxy]carbonyl]propyl]-2-oxoazetidinyl]propenamide (31) was prepared according to the same procedure as used for the synthesis of compound **32** and obtained as a colorless oil (32%) alone with **22j** (8%). Compound **31**: ^{1}H NMR δ 0.044 (s, 9 H), 0.046 (s, 9 H), 0.97–1.03 (m, 4 H), 1.97–2.06 (m, 1 H), 2.48–2.61 (m, 7 H), 0.99–4.04 (dq, $J_1 = 8.65$, $J_2 = 2.06$, 1 H), 4.15–4.23 (m, 4 H), 4.45–4.46 (d, $J = 2.43$, 1 H), 5.45 (s, 1 H), 5.85 (b, 1 H), 8.69 (b, 1 H); IR (TF) 3440, 3320, 2970, 1790, 1730, 1630, 1550, 1330, 1255, 1180, 865, 840 cm^{-1}; MS 518 (M$^+$), 266, 221, 193, 178, 106, 91. HRMS Calcd for $C_{22}H_{39}N_2O_6Si_2Cl$: 518.20352. Found: 518.2035.

Acknowledgment. We are grateful to Eli Lilly and Co. for the financial support of this research. We acknowledge Dr. C. M. Gasparski for preliminary discussions.

Photolysis of Tp′Rh(CN-neopentyl)(η^2-PhN=C=N-neopentyl) in Alkanes and Arenes: Kinetic and Thermodynamic Selectivity of [Tp′Rh(CN-neopentyl)] for Various Types of C–H Bonds

William D. Jones* and Edward T. Hessell

Contribution from the Department of Chemistry, University of Rochester, Rochester, New York 14627. *Received April 17, 1992*

Abstract: Irradiation of the carbodiimide complex [HB(3,5-dimethylpyrazolyl)$_3$]Rh(CNR)(PhN=C=NR) (R = neopentyl) in benzene, toluene, mesitylene, cyclopentane, cyclohexane, propane, or pentane solvent leads to both the clean elimination of the carbodiimide ligand and the formation of the C–H oxidative addition product [HB(3,5-dimethylpyrazolyl)$_3$]Rh(CNR)(R′)H. These products have been isolated as their chloride derivatives. Methane can be activated by exchange with the cyclohexyl derivative. The *n*-pentyl derivative [HB(3,5-dimethylpyrazolyl)$_3$]Rh(CNR)(*n*-pentyl)Cl crystallizes in monoclinic space group $P2_1/c$ with $a = 8.8865$ (28) Å, $b = 11.8016$ (30) Å, $c = 31.4597$ (14) Å, $\beta = 90.727$ (22)°, $Z = 4$, and $V = 3098$ (2) Å^3. Competitive studies show that both benzylic and aromatic C–H bonds react under conditions of kinetic control but that the aromatic activation products are thermodynamically preferred. Activation of primary alkane C–H bonds is preferred over secondary activation. This complex is found to be more selective than either [Cp*Rh(PMe$_3$)] or [Cp*Ir(PMe$_3$)]. The rates of reductive elimination of *n*-pentane, cyclopentane, cyclohexane, mesitylene, methane, and benzene have been measured and are used to establish relative Rh–R bond strengths for these ligands.

Introduction

The activation of C–H bonds by homogeneous transition-metal complexes continues to be an active area of research, and stable transition-metal activation products are now known for a number of systems.[1,2] The process leading to such products usually involves the photochemical or thermal generation of a high-energy coordinatively unsaturated intermediate (eq 1), which then inserts

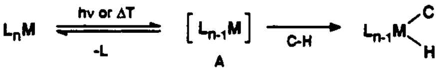

$$L_nM \underset{-L}{\overset{h\nu \text{ or } \Delta T}{\rightleftharpoons}} \underset{\mathbf{A}}{[L_{n-1}M]} \xrightarrow[C\text{-}H]{} L_{n-1}M{<}^{C}_{H} \quad (1)$$

into the C–H bond of an alkane. The insertion step can be viewed mechanistically as being similar to carbene insertion.[3,4] Much is known about the relative thermodynamic stabilities of various products derived from the oxidative addition of C–H bonds to unsaturated metal centers[5] ($\Delta G°$ of Figure 1) and, in turn, the relative strengths of the metal–carbon bonds in such products.[6]

---

[1] (a) Green, M. L. H.; O'Hare, D. *Pure Appl. Chem.* **1985**, *57*, 1897 and references therein. (b) Hackett, M.; Whitesides, G. M. *J. Am. Chem. Soc.* **1988**, *110*, 1449. (c) Seidler, P. F.; Wenzel, T. T.; Bergman, R. G. *J. Am. Chem. Soc.* **1985**, *107*, 4358. (d) Ghosh, C. K.; Graham, W. A. G. *J. Am. Chem. Soc.* **1987**, *109*, 4726. (e) Werner, H.; Hohn, A.; Dziallas, M. *Angew. Chem., Int. Ed. Engl.* **1986**, *25*, 1090. (f) Desrosiers, P. F.; Shinomoto, R. S.; Flood, T. C. *J. Am. Chem. Soc.* **1986**, *108*, 7964. (g) Baker, M. V.; Field, L. S. *J. Am. Chem. Soc.* **1987**, *109*, 2825–2826. (h) Belt, S. T.; Grevels, F.-W.; Klotzbücher, W. E.; McCamley, A.; Perutz, R. N. *J. Am. Chem. Soc.* **1989**, *111*, 8373–8382. (i) Maguire, J. A.; Goldman, A. S. *J. Am. Chem. Soc.* **1991**, *113*, 6706–6708.

[2] Barrientos, C.; Ghosh, C. K.; Graham, W. A. G.; Thomas, M. J. *J. Organomet. Chem.* **1990**, *394*, C31–C34. Ghosh, C. K.; Graham, W. A. G. *J. Am. Chem. Soc.* **1989**, *111*, 375–376. Ghosh, C. K.; Hoyano, J. K.; Krentz, R.; Graham, W. A. G. *J. Am. Chem. Soc.* **1989**, *111*, 5480–5481. Ghosh, C. K.; Graham, W. A. G. *J. Am. Chem. Soc.* **1987**, *109*, 4726–4727. Ghosh, C. K.; Rodgers, D. P. S.; Graham, W. A. G. *J. Chem. Soc., Chem. Commun.* **1988**, 1511–1512.

[3] Berry, M.; Elmitt, K.; Green, M. L. H. *J. Chem. Soc., Dalton Trans.* **1979**, 1950.

[4] (a) Crabtree, R. H. *Chem. Rev.* **1985**, *85*, 245. (b) Chetwynd-Talbot, J.; Grebenik, P.; Perutz, R. N. *Inorg. Chem.* **1982**, *21*, 3647.

[5] (a) Janowicz, A. H.; Bergman, R. G. *J. Am. Chem. Soc.* **1983**, *105*, 3929. (b) Buchanan, J. M.; Stryker, J. M.; Bergman, R. G. *J. Am. Chem. Soc.* **1986**, *108*, 1537. (c) Wax, M. J.; Stryker, J. M.; Buchanan, J. M.; Kovac, C. A.; Bergman, R. G. *J. Am. Chem. Soc.* **1984**, *106*, 1121. (d) Jones, W. D.; Feher, F. J. *J. Am. Chem. Soc.* **1984**, *106*, 1650. (e) Jones, W. D.; Feher, F. J. *Acc. Chem. Res.* **1989**, *22*, 91–100.

0002-7863/93/1515-554\$04.00/0

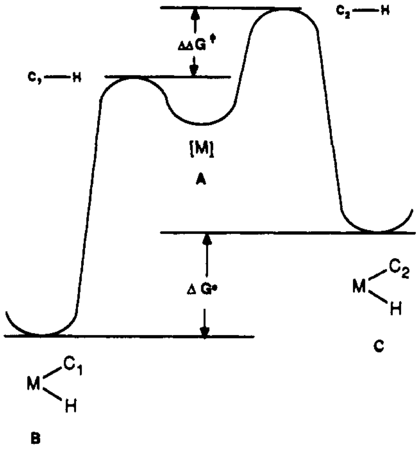

Figure 1. Free energy picture for competitive alkane activation.

Also, various studies have provided in-depth knowledge of the mechanism and intermediates along the pathway to C–H-activated products.[7]

Research has also focused on the study of the *kinetic* selectivity of coordinatively unsaturated intermediates for different types of alkane and arene C–H bonds and provides an estimate of the difference in activation barriers leading to C–H activated products ($\Delta\Delta G^{\ddagger}$ of Figure 1). Information of this type is important in relation to any catalytic cycle for hydrocarbon functionalization in which one typically desires formation of only one functionalized product from a substrate containing more than one type of C–H bond. Selectivity data for only a few systems is available, and an understanding of the factors contributing to high kinetic selectivity is limited.

A number of early reports of the activation of arene C–H bonds provide some initial insight into the kinetic selectivity in substituted arenes. Green et al. studied the photochemically induced activation of toluene and other substituted arenes with $Cp^*_2WH_2$[3] showing a preference for arene activation. Photolysis or thermolysis of Cp_2NbH_3 in the presence of substituted arenes and C_6D_6 resulted in incorporation of deuterium into the substituted arenes,[8] indicating that activation of the more electron deficient arenes was kinetically preferred, even though no intermediates were detected. Similarly, photolysis of $CpRe(PPh_3)_2H_2$ in a mixture of alkane or arene and benzene-d_6 resulted in incorporation of deuterium into arene C–H bonds faster than alkane C–H bonds.[9] Additionally, primary C–H bonds of alkanes reacted faster than secondary, and methane reacted faster than ethane, showing that substitution on the carbon is important and generally has a negative effect on rates of activation.

Most relevant to the research to be discussed here is the kinetic selectivity of coordinatively unsaturated intermediates of the type $[Cp^*M(PMe_3)]$ (M = Ir, Rh; $Cp^* = C_5Me_5$) generated photochemically from $Cp^*M(PMe_3)(H)_2$. Janowicz and Bergman compared the selectivity of $[Cp^*Ir(PMe_3)]$ for the different types of C–H bonds in arenes, alkanes, and cycloalkanes[5a] and witnessed only slight differences in reactivity (all of the relative rates were in the same order of magnitude). Jones and Feher measured the kinetic selectivity of $[Cp^*Rh(PMe_3)]$ for the different types of C–H bonds in toluene at −45 °C and witnessed a strong preference for activation of the meta and para C–H bonds relative to the ortho and benzylic bonds.[5d] A higher degree of selectivity was seen with the rhodium complex compared to the iridium complex.[10]

Scheme I. Products from Photolysis of **1** in Various Hydrocarbons

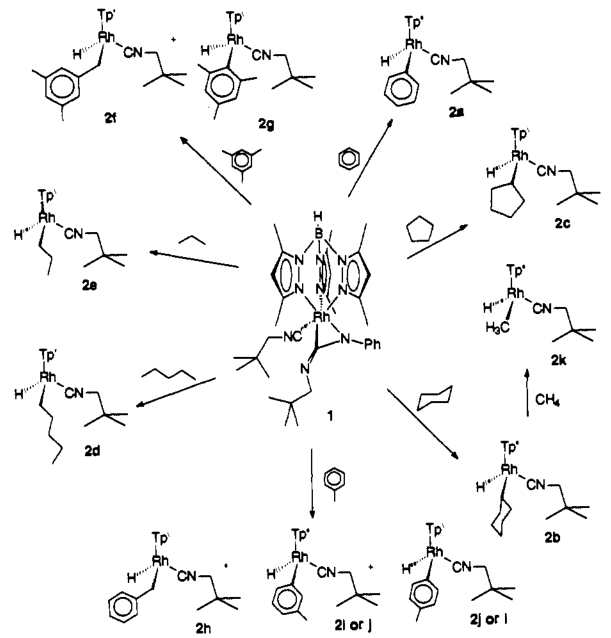

The scarcity of information relating to the kinetic selectivity of C–H bond activation by homogeneous transition metals can be attributed to the small number of systems possessing sufficiently stable C–H-activated products. In order to gain an accurate assessment of the true kinetic selectivity of any coordinatively unsaturated metal fragment, it is crucial that the products of C–H activation (B and C of Figure 1) do not interconvert at a rate comparable to the rate of their formation or the time required to obtain an estimate of their ratios. However, in order to ensure that the selectivity is actually kinetic in origin, it is necessary to be able to subsequently witness the approach to thermodynamic equilibrium. In many systems the C–H oxidative addition products undergo rapid exchange with solvent even at low temperature (eq 2), and hence the rapid approach to thermodynamic equilibrium makes the study of the kinetics of their initial formation impossible. Even for some systems that do have fairly stable activation products, efforts to conduct kinetic selectivity measurements at low temperatures, where the interconversion of products is slow, are often hampered by poor solubility of the complex precursors in alkane solvents.[11]

$$\overset{C_1}{\underset{H}{M}} + C_2\text{-}H \rightleftharpoons \overset{C_2}{\underset{H}{M}} + C_1\text{-}H \qquad (2)$$

In a previous paper it was reported that Tp'Rh(CNR)(η^2-PhN=C=NR) (**1**) (Tp' = hydrotris(3,5-dimethylpyrazolyl)borate, R = neopentyl) undergoes photochemical loss of carbodiimide to give a coordinatively unsaturated metal fragment capable of inserting into the C–H bonds of benzene to yield a stable product of type **2** (eq 3, R = Ph).[12] Complex **1** possesses excellent solubility in alkane solvents, even at temperatures below −20 °C. Also, the formation of C–H-activated products by photolysis of **1** is extremely rapid ($\Phi \approx 1$ in benzene at λ = 366 nm). For

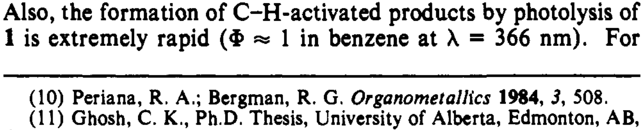

---

(6) (a) Nolan, S. P.; Hoff, C. D.; Stoutland, P. O.; Newman, L. J.; Buchanan, J. M.; Bergman, R. G.; Yang, G. K.; Peters, K. S. *J. Am. Chem. Soc.* **1987**, *109*, 3143. (b) Halpern, J. *Inorg. Chim. Acta* **1985**, *100*, 41. (d) Wasserman, E. P.; Moore, C. B.; Bergman, R. G. *Science* **1992**, *255*, 315–318. (e) Simões, J. A. M.; Beauchamp, J. L. *Chem. Rev.* **1990**, *90*, 629–688.

(7) (a) Periana, R. A.; Bergman, R. G. *J. Am. Chem. Soc.* **1986**, *108*, 7332. (b) Jones, W. D.; Feher, R. J. *J. Am. Chem. Soc.* **1982**, *104*, 4240. (c) Jones, W. D.; Feher, F. J. *J. Am. Chem. Soc.* **1986**, *108*, 4814.

(8) Klabunde, U.; Parshall, G. W. *J. Am. Chem. Soc.* **1972**, *94*, 9081.

(9) Jones, W. D.; Maguire, J. A. *Organometallics* **1986**, *5*, 590.

(10) Periana, R. A.; Bergman, R. G. *Organometallics* **1984**, *3*, 508.

(11) Ghosh, C. K., Ph.D. Thesis, University of Alberta, Edmonton, AB, Canada, 1988.

(12) Jones, W. D.; Hessell, E. T. *J. Am. Chem. Soc.* **1992**, *114*, 6087.

experiments conducted on an NMR tube scale, the complete conversion of **1** to products **2** generally occurs in less than 5 min. Importantly, the aryl hydride products are stable to further photolysis (i.e., light does not promote aryl hydride interconversions). Thus, it seemed possible to obtain rapid high conversions of Tp′Rh(CN-neopentyl)(η^2-PhN=C=N-neopentyl) to *alkyl* hydride products as indicated in eq 3 under conditions of kinetic control at low temperature. With this in mind, we decided to undertake a study of the relative kinetic selectivity of the coordinately unsaturated fragment [Tp′Rh(CN-neopentyl)][13] toward various types of alkyl, aryl, and benzylic C–H bonds (Scheme I) and to compare and contrast the observed selectivities with those reported from previous studies[5a,10] dealing with other coordinatively unsaturated metal centers.

Results

Synthesis and Characterization of Complexes Tp′Rh(H)(R)(CN-neopentyl). The photolysis experiments indicated in Scheme I were carried out in neat substrate to generate the indicated products. As these products were sensitive to chromatography on silica gel, the alkyl hydride complexes **2** were converted to the more stable alkyl chloride complexes **3** by reaction with a chlorine radical source such as carbon tetrachloride (eq 4). Complexes **2** were therefore commonly only characterized by ^{1}H NMR spectroscopy, while the chloride derivatives **3** were fully characterized by ^{1}H NMR, ^{13}C{^{1}H} NMR, IR, and elemental analysis.

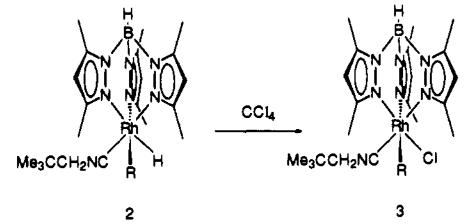

(4)

The synthesis of Tp′Rh(H)(Ph)(CN-neopentyl) involves photolysis (λ > 345 nm) of **1** in benzene, resulting in the rapid and quantitative formation of Tp′Rh(H)(Ph)(CN-neopentyl) (**2a**) and 1 equiv of PhN=C=N-neopentyl (**4**). The ^{1}H NMR spectrum of complex **2a** in benzene contains a resonance at δ −13.650 for the metal hydride (Table I) in addition to trace hydride resonances attributable to other products.[14] The six resonances observed in the ^{1}H NMR spectrum between δ 1.9 and 2.5, as well as the three resonances observed between δ 5.5 and 5.9, indicate that the complex is chiral at rhodium and probably contains an η^3-Tp′ ligand, as observed in the solid-state crystal structure of a related analog (vide infra). The IR spectrum possesses an absorption at 2178 cm^{-1}, which is typical for an isonitrile coordinated to a rhodium(III) metal center. The complex is indefinitely stable in solution at room temperature under an inert atmosphere, as is typical of most aryl hydride complexes of electron-rich metal centers.[5a,c,11] However, it is slowly converted to **3a** over a 3-day period by reaction in carbon tetrachloride.

The resonances in the ^{1}H NMR spectrum of **2a** in THF-d_8 associated with the phenyl protons are broad and unresolved at 25 °C (Figure 2). At −35 °C, however, all five of the protons are resolved as sharp multiplets, indicating that there is hindered rotation about the Rh–Ph bond in **2a**. Hindered rotation is not observed in the analogous Cp*Rh(PMe$_3$)(H)(Ph) or Cp*Ir(PMe$_3$)(H)(Ph), but it is seen in Cp*Rh(PMe$_3$)(Ph)Br,[15] showing that there is increased steric congestion at the metal for **2a** relative to the Cp* complexes. The steric congestion resulting from the neopentyl group of the isocyanide is not important, however, as the related Tp′Rh(H)(Ph)(CO)[11] also shows hindered rotation. The hindrance to rotation of the phenyl ring is related to the Tp′ ligand itself and provides evidence that Tp′ is more sterically demanding than Cp*.

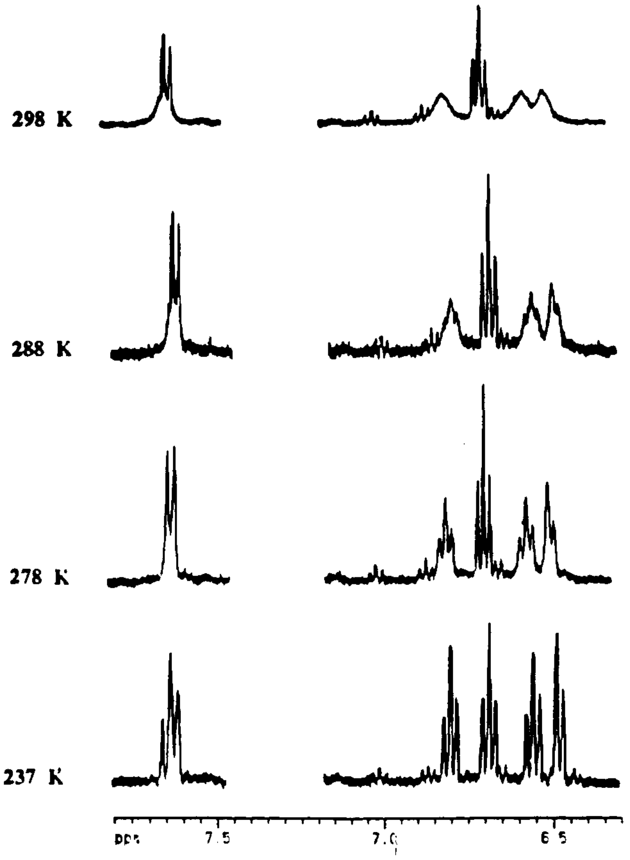

Figure 2. Variable temperature ^{1}H NMR of **2a** in THF-d_8. The doublet at δ 7.68 is an impurity and overlaps with the downfield ortho phenyl proton resonance of **2a**.

Photolysis of **1** in cyclohexane results in an immediate bleaching of the originally yellow solution. Removal of the solvent, followed by ^{1}H NMR analysis of the residue in cyclohexane-d_{12}, reveals the clean formation of Tp′Rh(H)(C_6H_{11})(CN-neopentyl) (**2b**). The ^{1}H NMR spectrum of **2b** contains a metal hydride resonance at δ −15.766 and a broad singlet at δ 1.42 attributable to the cyclohexyl group (Table I). If **2b** is left to stand in cyclohexane-d_{12} at 25 °C, conversion to the cyclohexyl deuteride is observed over 7 h with the concomitant formation of free cyclohexane. Over a period of 18 h, the products eventually decompose despite the presence of carbodiimide **4** in solution. Addition of carbon tetrachloride to a freshly prepared solution of **2b** results in the clean formation of the air-stable Tp′Rh(Cl)(C_6H_{11})(CN-neopentyl) (**3b**). A similar photolysis of **1** in cyclopentane affords the cyclopentyl hydride analog **2c**, which was also converted to its stable alkyl chloride **3c**.

Photolysis of **1** in *n*-pentane at 25 °C results in the clean formation of a single product possessing a hydride resonance at δ −15.367 (J = 24.8 Hz) in the ^{1}H NMR spectrum (Table I). The structural assignment of the product as Tp′Rh(H)(*n*-pentyl)(CN-neopentyl) (**2d**) is inferred from an X-ray crystal structure analysis of the corresponding alkyl chloride Tp′Rh(Cl)(*n*-pentyl)(CN-neopentyl) (**3d**) (Figure 3). Selected bond distances and angles for **3d** are listed in Table II. The η^3-coordination of the Tp′ ligand in **3d** is typical for a Rh(III) complex, and it is reasonable that this type of coordination is present in all of the corresponding alkyl hydrides **2**. Complex **2d** is stable for short periods in C_6D_{12} but slowly undergoes exchange with solvent as well as decomposition to a variety of products, as

---

(13) In this study, it has been assumed that all of the energy of the photon goes into labilization of the carbodiimide, producing the coordinatively unsaturated intermediate [Tp′Rh(CN-neopentyl)] in its ground state.

(14) Other metal–hydride products account for less than 10% of the total products as determined by NMR integration. A hydride at δ −13.384 (J = 22.2 Hz) belongs to the previously characterized Tp′Rh(H)(*o*-C_6H_4(N=C=NCH$_2$C(CH$_3$)$_3$)) (**5**) (see ref 12). Resonances at δ −13.676 and −13.625 are likewise suspected to be products arising from intramolecular C–H activation (meta or para) of **4**. Additionally a broad doublet centered at δ −14.1 is tentatively assigned as Tp′Rh(H)$_2$(CNCH$_2$C(CH$_3$)$_3$) (**6**). These products are typically observed in trace amounts in all photolyses of **1** in other hydrocarbons.

(15) Jones, W. D.; Feher, F. J. *Inorg. Chem.* **1984**, *23*, 2376–2388.

Table I. ^{1}H NMR Data for Complexes **2a–k**, Tp′Rh(CN-neopentyl)(R)H

entry	solvent	Rh–H	CNR	pzCH$_3$	pzH	other
2a R = Ph	C_6D_6	−13.650 *J* = 24 Hz	0.604 2.741	1.896 2.196 2.130 2.246 2.342 2.441	5.540 5.708 5.844	6.922 (br s, 1 H) 7.051 (t, *J* = 7.7 Hz, 1 H) 8.073 (br s, 1 H) other resonances not observed due to fluxional process
2b R = cyclohexyl	C_6D_{12}	−15.766 *J* = 25 Hz	0.981 3.259	2.052 2.136 2.221 2.278 2.358 2.390	5.379 5.522 5.564	1.422 (s, 10 H) methyne not observed
2c R = cyclopentyl	C_6D_{12}	−15.644 *J* = 25 Hz	0.970 3.116	2.156 2.218 2.294 2.295 2.350	5.466 5.569 5.617	1.511 (s, 8 H) methyne proton not observed
2d R = *n*-pentyl	C_6D_{12}	−15.367 *J* = 24.8 Hz	1.041 3.315	2.155 2.235 2.273 2.322 2.329 2.350	5.488 5.584 5.615	0.870 (t, *J* = 7 Hz, 3 H) 1.306 (m, 4 H) 1.582 (m, 2 H) 1.823 (m, 1 H)
2e R = *n*-propyl	C_6D_{12}	−15.336 *J* = 24.7 Hz	1.040 3.315	2.152 2.234 2.273 2.318 2.329 2.342	5.484 5.580 5.614	0.898 (t, *J* = 7 Hz, 3 H) other resonances for propyl group not observed
2f R = $CH_2C_6H_3$-3,5-Me_2	C_6D_6	−14.708 *J* = 23.2 Hz	0.505 2.551	2.181 2.186 2.305, 6 H 2.327, 6 H	5.606 5.621 5.863	2.703 (s, 3 H) 2.781 (s, 3 H) 3.229 (dd, J_1 = 10 Hz, J_2 = 2.7 Hz, 1 H) 3.907 (dd, J_1 = 10 Hz, J_2 = 4.0 Hz) 6.694 (s, 1 H) 7.506 (s, 2 H)
2g R = 1-mesityl	C_6D_6	−14.523 *J* = 21.2 Hz				
2k R = methyl	C_6D_6	−14.814 *J* = 24.4 Hz	0.659 2.745	2.195 2.238 2.306 2.401 2.534 2.538	5.610 5.687 5.799	1.236 (d, *J* = 2.0 Hz, 3 H)

Table II. Selected Intramolecular Bond Distances and Angles for Tp′Rh(Cl)(*n*-pentyl)(CN-neopentyl) (**3d**)

	Distances (Å)		
Rh–Cl	2.362 (1)	N7–C1	1.147 (5)
Rh–N1	2.226 (4)	N7–C7	1.465 (6)
Rh–N3	2.100 (4)	C2–C3	1.535 (6)
Rh–N5	2.063 (3)	C3–C4	1.541 (6)
Rh–C1	1.906 (5)	C4–C5	1.503 (7)
Rh–C2	2.105 (4)	C5–C6	1.527 (7)
	Angles (deg)		
Cl–Rh–N1	91.6 (1)	N3–Rh–C1	178.4 (2)
Cl–Rh–N3	92.1 (1)	N3–Rh–C2	92.8 (2)
Cl–Rh–N5	178.2 (1)	N5–Rh–C1	90.8 (2)
Cl–Rh–C1	87.4 (1)	N5–Rh–C2	93.2 (1)
Cl–Rh–C2	87.2 (1)	C1–Rh–C2	88.7 (2)
N1–Rh–N3	84.9 (1)	Rh–N1–N2	116.2 (2)
N1–Rh–N5	88.1 (1)	C1–N7–C7	175.2 (5)
N1–Rh–C1	93.6 (2)	Rh–C1–N7	179.0 (4)
N1–Rh–C2	177.3 (1)	Rh–C2–C3	117.1 (3)
N3–Rh–N5	89.7 (1)		

determined from the ^{1}H NMR spectrum.[16] A similar photolysis of **1** in pentane at low temperature (−45 °C) showed no evidence for the formation of kinetic products arising from activation of the secondary bonds of pentane.

Photolysis of **1** as a suspension in liquid propane at −45 °C results in incomplete conversion of **1** to Tp′Rh(H)(*n*-propyl)(CN-neopentyl) (**2e**). As might be expected, the chemical shifts of the Tp′ ligand and isocyanide ligand of **2e** are virtually identical to those of **2d** (Table I). The doublet resonance at δ −15.336 is clearly consistent with the activation of a primary C–H bond, and no evidence for the activation of the secondary bond was observed. Resonances for the *n*-propyl group could not be clearly assigned and are assumed to be buried under the resonances for the Tp′ ligand. Because of the limited solubility of **1** in propane, it was not practical to attempt a preparative scale reaction in order to isolate the alkyl chloride analog.

Photolysis of **1** in mesitylene at 25 °C results in the formation of two hydride-containing products in a 3:1 ratio. The major product is clearly identified as Tp′Rh(H)[$CH_2C_6H_3$-3,5-$(CH_3)_2$](CN-neopentyl) (**2f**) by the ^{1}H NMR spectrum C_6D_6, which shows two doublet of doublet resonances for the diastereotopic benzylic protons (Table I). The minor hydride resonance at δ −14.523 is tentatively assigned to Tp′Rh(H)[C_6H_2-2,4,6-$(CH_3)_3$](CN-neopentyl) (**2g**), but the chemical shift for this resonance appears to be at higher field than expected for an aryl hydride, an effect that might be associated with extreme steric hindrance. This minor product was not observed in the competitive kinetic selectivity experiments with toluene (vide infra). Addition of carbon tetrachloride to a freshly prepared solution of the hydride products allows for isolation and characterization of complex **3f**. However, all attempts to convert **2g** to its corresponding aryl chloride resulted in the formation of a product tentatively identified by ^{1}H NMR spectroscopy as Tp′Rh(Cl)$_2$(CN-neopentyl) (**7**) (see

---

[16] The ^{1}H NMR spectrum of the solution of **2c** in C_6D_{12} after standing at 25 °C for 4 h shows doublet resonances in the hydride region at δ −13.875 (*J* = 22.2 Hz) and −14.092 (*J* = 24.7 Hz). The former resonance is attributed to **5** and the latter to **6**.

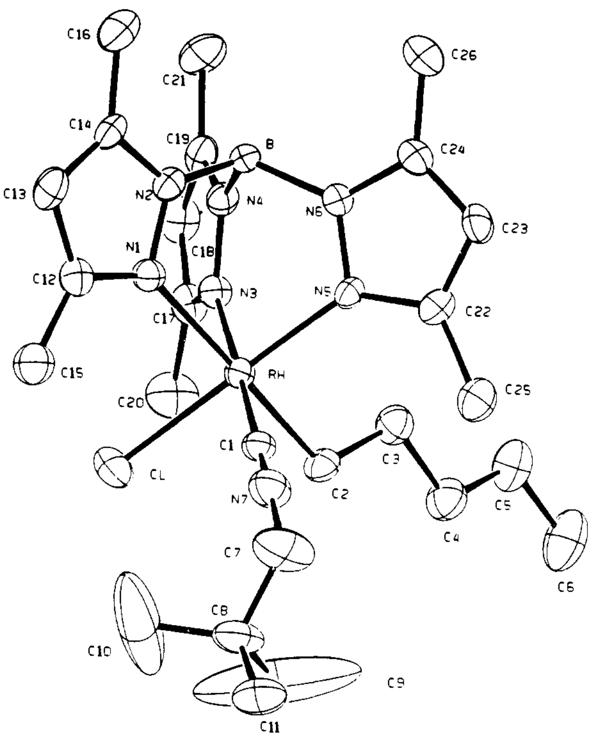

Figure 3. ORTEP drawing of Tp′Rh(Cl)(*n*-pentyl)(CN-neopentyl) (**3d**). Ellipsoids are shown at the 50% probability level, and hydrogen atoms have been omitted for clarity.

Table III. ^{1}H NMR Data for **2h–j**

T, °C	solvent	hydride (J_{RhH}, Hz)	ratio	compd
25	C_6D_6	−14.754 (23.2)	2	**2h**
		−13.678 (25.1)	4	**2j**
		−13.663 (24.5)	3	**2i**
		−13.384 (22.2)	1	**5**
−35	C_7H_8:C_7D_8, 3:1	−14.755 (24 Hz)	3.0	**2h**
		−13.686 (25 Hz)	3.2	**2j**
		−13.666 (25 Hz)	3.2	**2i**
		−13.396 (23 Hz)	1.0	**5**

Experimental Section). Complex **2f** is stable for hours in benzene solution at 25 °C. This surprising result will be discussed further in relation to the competitive kinetic selectivity study.

The photolysis of **1** in toluene at 25 °C gives three major hydride-containing products in a 2:4:3 ratio (in order of high-field to low-field, Table III), along with the usual trace amounts of carbodiimide activation products.[14] Because of the number of products formed in this reaction, it was not possible to fully characterize each species individually by ^{1}H NMR spectroscopy, although reasonable assignments can be made by comparison of the chemical shifts of the hydride resonances in the ^{1}H NMR spectrum to those of examples characterized above. The resonance at δ −14.745 is assigned as Tp′Rh(H)($CH_2C_6H_5$)(CN-neopentyl) (**2h**) by analogy to **2f**. The hydride resonances at δ −13.678 and −13.663 are assigned to Tp′Rh(H)[C_6H_4(3-CH_3)](CN-neopentyl) (**2i**) and Tp′Rh(H)[C_6H_4(4-CH_3)](CN-neopentyl) (**2j**), respectively. The approximately equal intensity of these resonances indicates a kinetic preference for activation of toluene at the para position relative to the meta position. Heating of the sample at 100 °C for 12 h results in complete conversion of all initial products to a statistical 2:1 mixture of **2i** and **2j**. The major difference between this result and those of previous studies by Jones and Feher[5d] and Green[3] is the large kinetic preference for benzylic activation.

If the photolysis is conducted at −35 °C in a 3:1 toluene:toluene-d_8 solvent mixture, the selectivity for the methyl C–H bonds of toluene increases (Table III). Although not shown in the table, resonances for the carbodiimide activation products now account for 21% of the hydride products.[14] This experiment clearly indicates the effect that temperature can have on the observed kinetic selectivities, especially with experiments involving vastly different types of C–H bonds.

Table IV. Rates of Reductive Elimination of RH from Tp′Rh(CN-neopentyl)(R)H in C_6H_6 at 23 °C

R	k_{re}(RH), s^{-1}	$\Delta G_{re}^{\ddagger}$, kcal/mol
phenyl	1.13×10^{-10} [a]	30.99[a]
α-mesityl	6.66 (43) × 10^{-6}	24.49 (4)
methyl	3.41 (13) × 10^{-5}	23.52 (3)
n-pentyl	2.15 (10) × 10^{-4}	22.43 (3)
cyclopentyl	1.79 (26) × 10^{-3}	21.18 (9)
cyclohexyl	1.24 (10) × 10^{-3}	21.40 (5)

[a] Calculated from Eyring plot data in ref 12.

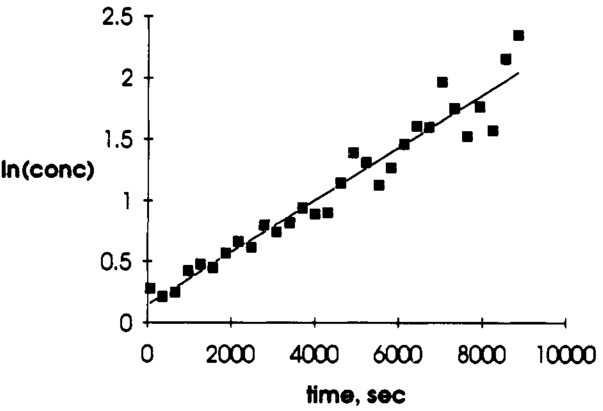

Figure 4. Plot of the conversion of Tp′Rh(CN-neopentyl)(*n*-pentyl)H to Tp′Rh(CN-neopentyl)(Ph)H at 23 °C.

Quenching of the hydrides with carbon tetrachloride followed by preparative thin-layer chromatography allowed for isolation of **3h**. The complex slowly decomposes over time, so a complete characterization was not possible. Complexes **3i** and **3j** could only be isolated as a mixture, and even in this case several other products were present.

Only two of the alkanes investigated failed to react with **1** under photochemical conditions. Complex **1** possesses poor solubility in neopentane at −18 °C, and so the photolysis was conducted in a 1:1 pentane:neopentane solvent mixture. The ^{1}H NMR spectrum of the mixture after photolysis showed only **2d**. An analogous result was reported by Ghosh and Graham with the photolysis of Tp′Rh(CO)$_2$ in neat neopentane.[11]

The large degree of selectivity for primary vs secondary C–H bonds observed in the photolysis experiments with *n*-pentane and *n*-propane suggested that it might be possible to activate methane in cyclohexane. Photolysis of a cyclohexane solution of **1** under 1 atm of methane, however, produced only **2b**. Methane activation was ultimately achieved, however, by pressurization of this solution with methane (2300 psi) for 18 h at room temperature. Loss of cyclohexane from **2b** occurs readily under these conditions (vide infra), and oxidative addition of methane proceeds to completion to give **2k**. Removal of the solvent under vacuum followed by dissolving the solution in benzene allows observation of the new hydride resonance at δ −14.814 (d, J = 24.4 Hz) as well as other resonances for Tp′Rh(CN-neopentyl)(Me)H. Others have also succeeded in exchanging a cyclohexyl hydride with methane at higher pressures.[1d,5c]

The rates of reductive elimination of alkane from complexes **2b**, **2c**, **2d**, **2f**, and **2k** were also measured by dissolving samples of each complex in C_6H_6 and monitoring the rate of conversion to **2a** by ^{1}H NMR spectroscopy. Under these conditions, the elimination of the alkane is irreversible. Table IV summarizes the rate constants k_{re}(RH) obtained from first-order plots of the extent of reaction (e.g., Figure 4), along with the activation energies for the reductive eliminations at 23 °C ($\Delta G_{re}^{\ddagger}$).

Competitive Selectivity Experiments. With a number of the C–H-activated products **2** fully characterized by ^{1}H NMR spectroscopy, several competitive kinetic selectivity experiments

Table V. Kinetic Selectivity Data

run	substrates	solvent ratio (V_1:V_2)	T (°C)[d]	irrad time (min)	integrated area, (I_1:I_2)	k_1/k_2[e]
1	benzene:α-mesitylene	1:1	−15	4.5	2.0:1.0[a,f]	2.0:1.0
2	benzene:pentane	2:1	−15	7.0	3.0:1.0[a]	4.7:1
3	pentane:cyclohexane	1:1	−15	10.0	6.7:1.0[a]	15:1
4	cyclopentane:cyclohexane	1:1	−20	5.0	1.2:1.0[b]	1.7:1
5	propane:pentane	1.4:1[c]	−45	15.0	1.6:1.0[a]	1:1

[a] Determined from integration of hydride resonances. [b] Determined from integration of pyrazolylH resonances at δ 5.628 (**2c**) and 5.645 (**2b**). [c] Based on assumption that density of propane is roughly equal to that of pentane at −45 °C. [d] Temperature of sample during photolysis. All ^{1}H NMR spectra were collected at −15 °C. [e] Determined from eq 5. [f] For methyl protons of mesitylene.

Table VI. Relative Kinetic Selectivities of Coordinatively Unsaturated Metal Centers[a]

substrate	site	[Tp′Rh(CNR)] (−15 °C)	[Cp*Rh(PMe$_3$)] (−60 °C)	[Cp*Ir(PMe$_3$)] (−60 °C)
benzene		69	19.5	3.9
mesitylene	methyl	36		
	aryl	12		
pentane	1°	15		
	2°	0[b]		
hexane	1°		5.9	2.7
	2°		0[b]	0.2
propane	1°	15	2.6	1.5
	2°	0[b]	0[b]	0.3
cyclohexane		1.0	1.0	1.0
cyclohexane		1.7	1.8	1.1

[a] Ratios are calculated on a per-hydrogen basis. [b] Not detected, but possibly present at less than 5% of total product.

were conducted, as shown in Table V. In a typical experiment, **1** was dissolved in a solvent mixture of the two substrates to be studied in an NMR tube which was flame sealed under 1 atm of N_2.[17] The sample was irradiated with $\lambda > 345$ nm at low temperature and then quickly transferred to the precooled NMR probe, where a ^{1}H NMR spectrum was obtained (<2 min). Under these conditions the kinetic products may be observed, since the rates of reductive elimination are very slow. Subsequent ^{1}H NMR spectra were collected over the next 45 min to verify that the product ratios did not change significantly under the conditions of the experiment. Continued photolysis of the products at low temperature after complete conversion of **1** did not affect the observed product ratios (entries 1 and 4). Entry 5 is the only example in which the products were not observed directly in the substrate solution after the photolysis. Instead, the solvents were evaporated in vacuo at 0 °C after completion of the photolysis, and the residue was dissolved in C_6D_{12}. In this case the rate of interconversion of the products is assumed to be negligible at the low temperatures used during the solvent evaporation and NMR sample preparation.

The selectivities reported in Table V were used in eq 5 to calculate the relative rates (k_1 vs k_2) at which the coordinatively unsaturated intermediate [Tp′Rh(CN-neopentyl)] reacts with two types of C–H bonds. For eq 5, I_1/I_2 = integration ratio; H_2/H_1 = ratio of number of C–H bonds; V_2/V_1 = ratio of solvent volumes; d_2/d_1 = solvent density ratio; MW_1/MW_2 = ratio of molecular weights. It should be noted that eq 5 contains a statistical factor which accounts for the relative number of each type of C–H bond available for reaction, and hence the kinetic ratios are *per C–H bond*.[18]

$$\frac{k_1}{k_2} = \left(\frac{I_1}{I_2}\right)\left(\frac{H_2}{H_1}\right)\left(\frac{V_2}{V_1}\right)\left(\frac{d_2}{d_1}\right)\left(\frac{\mathrm{MW}_1}{\mathrm{MW}_2}\right) \qquad (5)$$

It was possible to observe approaches to thermal equilibrium in several of the runs reported in Table V. Heating of the initial products from entry 1 at 60 °C for 1.5 h results in total conversion of **2f** to **2a**. In entries 2 and 3 of Table V, product interconversions could be seen upon warming the mixture to 25 °C over several hours. For entry 4, no appreciable change in the product ratios was observed at 25 °C. Instead, a general slow decomposition of the products over 10 h occurred, as is common for all of the alkylhydridorhodium complexes **2**. It is quite possible that the kinetic selectivity is coincidentally similar to the thermodynamic selectivity, as has been determined for the related Cp*Ir(PMe$_3$)(H)(R) system,[5b] which favored primary activation products exclusively under the conditions of the experiment.

Discussion

Photolysis of **1** serves as an efficient method for the generation of [Tp′Rh(CNR)], which is reactive toward a variety of aliphatic and aromatic C–H bonds, as shown in Scheme I. This method of generation of the unsaturated intermediate also allows for the determination of kinetic selectivities for various C–H bonds. The selectivities calculated in Table V were used to construct Table VI, in which the relative rates of reaction for each type of C–H bond are compared to each other (the rate of cyclohexane activation being assigned an arbitrary rate of 1.0). Also included in Table VI are the results from the two most relevant previous studies involving similar coordinatively unsaturated intermediates.[10] The selectivity for a methane/benzene competition could not be observed experimentally but was assumed to be twice that seen in the benzene/pentane competition.[9]

Comparison of the results of the present study with those obtained earlier by Bergman, Jones, et al. shows that the general order of reactivity of different types of C–H bonds with the intermediate [Tp′Rh(CN-neopentyl)] is remarkably similar to both [Cp*Rh(PMe$_3$)] and [Cp*Ir(PMe)$_3$] (i.e., Ph–H ≫ 1° alkyl > cycloalkyl). Thus, it appears that the factor or factors controlling selectivity for *different types* of C–H bonds is not dependent on either the ligands attached to the metal or the metal itself. However, it should be kept in mind that there is a distinct similarity between the steric demands and electronic interactions of the Tp′ and Cp* ligands, although, as was previously mentioned with regard to the ^{1}H NMR spectrum of **2a**, the sterics of the Tp′ ligand are generally more demanding than those of Cp*. This may explain why [Tp′Rh(CN-neopentyl)] does not activate neopentane while [Cp*Rh(PMe$_3$)] does. Neither of the rhodium intermediates gives observable products arising from activation of secondary C–H bonds in acyclic alkanes. This result is nonconclusive with respect to kinetic selectivity, since it is quite possible that some secondary activation occurs but that the product alkyl hydrides are both kinetically and thermodynamically unstable under the conditions of the experiment.[7a] With regard to the degree of selectivity between different types of C–H bonds, the intermediate [Tp′Rh(CN-neopentyl)] is slightly more discriminating than [Cp*Rh(PMe$_3$)] with respect to both benzene vs pentane and pentane vs cyclohexane activation, which, in turn,

---

(17) Entries 1–5 of Table V were designed so that (1) at least one of the substrates under study was available as a deuteride so that a small amount could be added as a lock solvent and (2) the solvent mixture did not freeze under the conditions of the experiment. Also, effort was made to adjust the ratio of the two substrate hydrocarbons in the mixture to make the integration of the hydride resonances of the products after photolysis approximately equal in the ^{1}H NMR spectrum (a measure undertaken to provide more accurate integration ratios). The one exception is entry 3, where a large cyclohexane:pentane solvent ratio would produce a solution that freezes at −15 °C.

(18) In the calculation for entry 5, the density of propane was estimated to be equal to that of pentane. This assumption is not unreasonable, since the densities of lower linear alkanes increase only slightly with increasing chain length (pentane–octane, 0.626–0.703). Although no formal calculation of error was performed for the integrations listed in Table V, reproducibility was very good for all of the entries except 3, for which the reproducibility was on the order of ±2.

Scheme II. Free Energy Reaction Coordinate for Tp′Rh(CN-neopentyl)(R)H Complexes at 23 °C

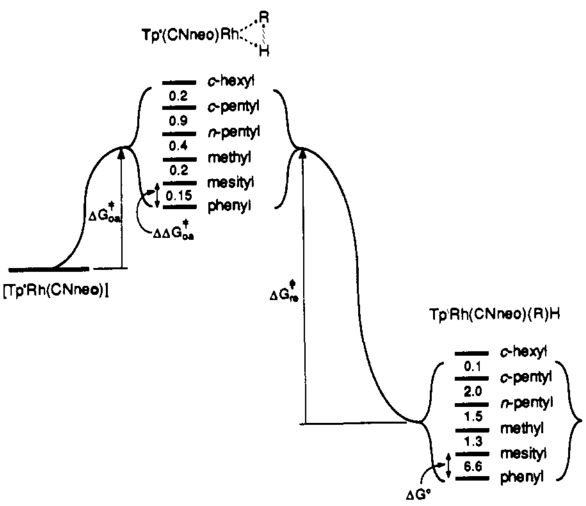

was more discriminating than [Cp*Ir(PMe$_3$)].

Another interesting point concerns the high degree of selectivity observed by both rhodium systems as compared to iridium, despite the fact that the thermodynamic stability of the product alkyl hydrides **2** is closer to the iridium complexes Cp*Ir(H)(R)(PMe$_3$) (**7**). Bergman has suggested that the greater selectivity observed with the intermediate [Cp*Rh(PMe$_3$)] over that of [Cp*Ir(PMe$_3$)] is related to the thermodynamic stability of the alkyl hydride complexes[10] (the less exothermic activation should be more selective). Complexes Cp*Rh(H)(R)(PMe$_3$) (R = alkyl) (**8**) are only stable below −20 °C, whereas the corresponding complexes **7** are typically stable at room temperature. Complexes **2a–e** are clearly more stable than complexes **8** (being stable at 25 °C for several hours), and yet the kinetic selectivity of [Tp′Rh(CN-neopentyl)] is slightly greater than that of [Cp*Rh(PMe$_3$)]. Therefore, greater kinetic selectivity is not necessarily associated with less stable alkyl hydride products (i.e., a less exothermic C–H activation reaction). It could also be argued that while increased steric factors in the Tp′Rh case result in higher selectivity (vs Cp*Rh), electronic factors provide greater stability to the alkyl hydride products.

The most significant result obtained from the present study concerns the kinetic selectivity observed for the benzylic C–H bonds in mesitylene. It has been proposed that the order of thermodynamic stability of M–C bonds is as follows[19]

$$\text{M–Ph} \gg \text{M–vinyl M–CH}_3 > \text{M–CH}_2\text{R} > \text{M–CHR}_2 > \text{M–CH}_2\text{Ph}$$

The strong preference for activation of benzylic C–H bonds by Tp′Rh over all other types of bonds except benzene appears at first to contradict the notion that the kinetic selectivity for a C–H bond follows the thermodynamic stability of the M–C bonds of the product alkylhydridometal complexes.

Table VII. Selectivities and Thermodynamics for Formation of Tp′Rh(CN-neopentyl)(R)H

R	k_{rel}(RH)[a]	$\Delta\Delta G_{oa}^{\ddagger}$, kcal/mol	ΔG°,[b] kcal/mol	D_{rel}(R–H),[c] kcal/mol
phenyl	1	0	0	0
α-mesityl	1.33	0.15	6.6	31.6
methyl	~2.3[d]	~0.4[d]	7.9[d]	13.9[d]
n-pentyl	4.7	0.80	9.4	21.4
cyclopentyl	24.8	1.7	11.5	27.0
cyclohexyl	35.2	1.8	11.4	26.9

[a] $k_{rel} = k_{oa}(C_6H_6)/k_{oa}(RH)$ for oxidative addition of a molecule of substrate, measured at −15 °C. [b] Relative to Tp′Rh(CN-neopentyl)(Ph)H. [c] Bond strengths relative to D_{Rh-Ph} in Tp′Rh(CN-neopentyl)(Ph)H. $D_{rel} = D_{Ph-H} - D_{C-H} + \Delta G^\circ$. [d] Calculated by assuming methane to be twice as reactive as *n*-pentane.

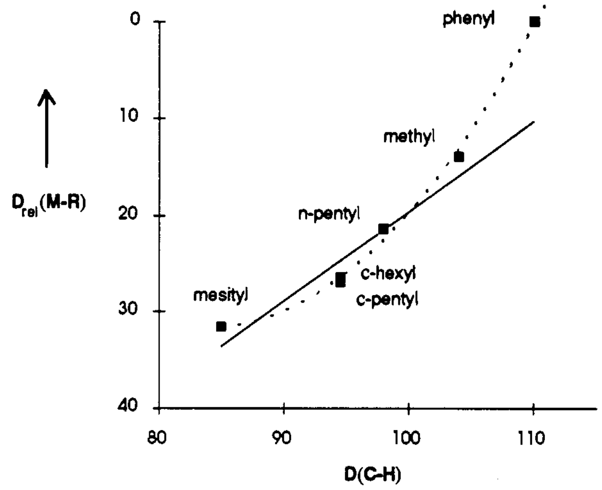

Figure 5. Plot of relative metal–carbon bond strength vs carbon–hydrogen bond strength (kcal/mol). $D_{rel}(M-R) = D_{M-Ph} - D_{M-R}$. The solid line has a slope of 0.96 and is fit to the sp^3 hybridized hydrocarbons only (phenyl is excluded). The dotted line is a parabolic fit of all data ($y = m(x - h)^2 + k$, where $m = -0.459$, $h = 83.85$, and $k = 31.68$).

Combination of the kinetic selectivity data with the reductive elimination data for compounds **2** allows the determination of the relative M–C bond strengths for these complexes, as shown in Scheme II. The selectivities for oxidative addition of a substrate to [Tp′Rh(CN-neopentyl)] can be referenced to benzene and converted to differences in free energies of activation ($\Delta\Delta G_{oa}^{\ddagger}$), as listed in Table VII. Using eq 6, the free energies for reductive

$$\Delta G^\circ = \Delta G_{re}^{\ddagger}(\mathbf{2a}) + \Delta\Delta G_{oa}^{\ddagger}(RH) - \Delta G_{re}^{\ddagger}(RH) \qquad (6)$$

elimination of RH ($\Delta G_{re}^{\ddagger}$) can be combined with the $\Delta\Delta G_{oa}^{\ddagger}$ values to give relative free energies for compounds **2** (ΔG°). Combining the ΔG° values with the hydrocarbon bond strengths (D_{R-H})[20] gives Rh–R bond strengths relative to the Rh–phenyl bond (eq 7), as summarized in Table VII.[21] Methane can be

$$D_{rel}(M-R) = D_{Rh-Ph} - D_{Rh-R} = \Delta G^\circ + D_{Ph-H} - D_{R-H} \quad (7)$$

included in this comparison even though its kinetic selectivity vs another alkane could not be measured. The range of kinetic selectivities observed is very slight, and it can be approximated that methane would be about twice as reactive as *n*-pentane on the basis of selectivities seen in other systems.[9]

Comparison of these values provides insight into the origins of the thermodynamic selectivities. First, the metal–phenyl bond is 27 kcal/mol stronger than the metal–secondary carbon bond, as compared with only 21 kcal/mol stronger than the metal–primary carbon bond. This greater relative strength of the metal–phenyl bond (~6 kcal/mol) is not fully offset by the fact that it is easier to break a secondary C–H bond relative to a primary C–H bond (by 3.5 kcal/mol), and, consequently, primary C–H activation is thermodynamically preferred. Note that the two metal–secondary carbon bond strengths are about the same.

In the case of mesitylene, the metal–phenyl bond is now ~32 kcal/mol stronger than the metal–benzylic bond. The difference in the benzene C–H bond vs the benzylic mesitylene C–H bond (~25 kcal/mol) is still insufficient to dominate the thermodynamics, and one finds that the mesityl complex **2f** is still thermodynamically less stable than the phenyl complex **2a**. The

---

(19) *Activation and Functionalization of Alkanes*; Hill, C. L., Ed.; John Wiley and Sons: New York, 1989; Chapter IV, p 111.

(20) Bond strengths were taken from: Benson, S. W. *Thermochemical Kinetics*; John Wiley and Sons: New York, 1976. D_{Ph-H} = 110 kcal/mol; $D_{methyl-H}$ = 104 kcal/mol; $D_{n\text{-pentyl}-H}$ = 98 kcal/mol; $D_{cyclohexyl-H} = D_{cyclopentyl-H}$ = 94.5 kcal/mol; $D_{mesityl-H}$ = 85 kcal/mol.

(21) In these calculations, it is assumed that differences in the entropies of these reactions are identical and, therefore, cancel in the calculation of enthalpy differences from free energy differences. For a fuller discussion of the validity of this calculation, see ref 5d.

interesting features, however, are that the difference in the C–H bond strengths is now barely exceeded by the difference in M–R bond strengths (by 28%) and that the extrapolation from the relative C–H bond strengths has "leveled off". These comparisons can be most easily seen by plotting D_{rel}(M–R) vs D(C–H) (Figure 5). The metal–benzyl bond can be seen to be stronger than expected on the basis of this plot (i.e., D_{rel} is smaller than would be predicted by extrapolation from the alkyl data) and consequently is assigned as the source of the high thermodynamic preference for benzylic activation. The origin of this increased bond strength is not apparent at the present time.

One can fit the data for only the sp^3 hybridized carbons to a line, giving a slope of 0.96, as shown by the solid line in Figure 5. Other workers have also noted nearly linear correlations of M–X and X–H bond strengths.[22] In this type of correlation, the strength of the metal–phenyl bond is apparently the only one that does not fit well, although the origin of this increased bond strength is not apparent at the present time. The electronegativity of the phenyl group may be adding an electronic influence on the bond strength that causes it not to fit the correlation. While the errors in these data are probably on the order of 1–2 kcal/mol, all of the bond strengths more closely fit a parabola (Figure 5, dotted line), and it may be that the correlation of metal–carbon bond strengths with carbon–hydrogen bond strengths is not linear. One observation that must be accommodated, however, is that there is a thermodynamic preference for breaking the stronger C–H bonds within a series of alkanes. For any given hydrocarbon, a line of slope = 1 can be drawn passing through this point in Figure 5, and all hydrocarbons lying below the line will be thermodynamically more favored whereas those lying above the line will be thermodynamically less favored.

It is worthwhile to point out that there are several other reports of benzylic activation being competitive with aromatic activation,[23] including the case of [Cp*Ir(PMe$_3$)].[5a] Also, Halpern has found that the cobalt–benzyl bond in (py)(saloph)Co(CH$_2$Ph) is intermediate in strength between the cobalt–*n*-propyl bond and the cobalt–iso-propyl bond, despite the large difference in C–H bond strengths.[24] Our earlier studies indicating a lack of reactivity of toluene benzylic C–H bonds with [Cp*Rh(PMe$_3$)] required indirect product analysis by reaction with CHBr$_3$ to form bromide derivatives and consequently may not have reflected the true kinetic product distribution.

Conclusions

The kinetic selectivity of the coordinatively unsaturated intermediate [Tp′Rh(CN-neopentyl)] for activation of different types of C–H bonds has been probed by photolysis of Tp′Rh(CN-neopentyl)(η^2-PhN=C=N-neopentyl) in hydrocarbon mixtures. The kinetic selectivity of [Tp′Rh(CN-neopentyl)] for primary alkyl vs secondary cycloalkyl C–H bonds and benzene vs primary alkyl C–H bonds is slightly better than that observed with the intermediate [Cp*Rh(PMe$_3$)], thus indicating that the kinetic selectivity of the intermediates is not necessarily related to the thermodynamic stability of the alkylhydridometal products. Activation of the benzylic C–H bonds of mesitylene is favored over that of the primary C–H bonds in pentane by 2:1 and is attributed to a stronger metal–mesityl bond than was earlier anticipated. The strong preference for benzylic activation is the only example in which the kinetic selectivity for the C–H bond is not inversely proportional to the C–H bond strength.

Experimental Section

General. All operations and routine manipulations were performed under a nitrogen atmosphere, either on a high vacuum line using modified Schlenk techniques or in a Vacuum Atmospheres Corporation dri-lab. Tetrahydrofuran, benzene, and toluene were distilled from dark purple solutions of benzophenone ketyl. Benzene-d_6, THF-d_8, and toluene-d_8 were distilled under vacuum from dark purple solutions of benzophenone ketyl and stored in ampules with Teflon-sealed vacuum line adapters. Alkanes were stirred over H_2SO_4, washed with aqueous acidic $KMnO_4$ and water, and distilled from purple tetraglyme/benzophenone ketyl solutions.

All ^{1}H NMR spectra were recorded on Bruker AMX400 or WP200 NMR spectrometers. All chemical shifts are reported in ppm (δ) relative to tetramethylsilane and referenced to the chemical shifts of residual solvent resonances (C_6H_6, δ 7.15; THF, δ 3.58, 1.73; toluene, δ 2.09). All temperatures for variable temperature NMR spectroscopy were calibrated relative to the chemical shift differences in the NMR spectra of known standards (4% methanol in methanol-d_4). All kinetics plots and least-squares error analyses of rate data were done using Microsoft Excel. Analyses were obtained from Desert Analytics. The preparation of Tp′Rh(CN-neopentyl)(η^2-PhN=C=N-neopentyl) (**1**) has been described previously.[12] Silica gel plates used in the preparative thin-layer chromatography were purchased from Analtech and contained a fluorescent indicator.

Preparation of Tp′Rh(Cl)(C_6H_{11})(CNCH$_2$C(CH$_3$)$_3$) (3b). A stirred bright yellow solution of 65 mg (0.095 mmol) of **1** in 5 mL of cyclohexane was irradiated with $\lambda > 345$ nm for 20 min at 10 °C. To the resulting pale yellow solution was added under inert conditions 1 mL of carbon tetrachloride. The temperature was maintained at 10 °C for 2 h, after which point the solvent was evaporated in vacuo. The crude product was separated from **4** by preparative thin-layer chromatography (500-μm silica gel on 20 × 20 cm^2 glass plate, 9:1 hexane:THF mobile phase). Yield: 38 mg (65%) as a white solid. ^{1}H NMR (C_6D_6): δ 0.706 (s, 9 H, C(CH$_3$)$_3$), 2.113 (s, 3 H, pzCH$_3$), 2.177 (s, 3 H, pzCH$_3$), 2.213 (s, 3 H, pzCH$_3$), 2.484 (s, 3 H, pzCH$_3$), 2.690 (s, 2 H, NCH$_2$), 2.766 (s, 3 H, pzCH$_3$), 3.090 (s, 3 H, pzCH$_3$), 4.980 (br s, 1 H, RhCH), 5.569 (s, 1 H, pzH), 5.650 (s, 1 H, pzH), 5.686 (s, 1 H, pzH). Other resonances for the cyclohexyl group were broad and unresolved due to fluxionality within the ring, ^{13}C{^{1}H} NMR (C_6D_6): δ 12.263, 12.870, 13.146, 14.674 (pzCH$_3$), 14.810, 16.312 (cyclohexylCH$_2$), 26.726 (C(*C*H$_3$)$_3$), 28.316 (pzCH$_3$), 30.066, 30.152 (cyclohexylCH$_2$), 31.349 (*C*(CH$_3$)$_3$), 31.864 (pzCH$_3$), 37.170 (br s, RhCH), 56.328 (NCH$_2$), 106.549, 107.781, 109.192 (pzCH), 142.454, 142.659, 144.453, 150.898, 150.932, 152.935 (pzC$_q$). IR (KBr): 2531 (B–H), 2206 (CNR) cm^{-1}. Anal. Calcd (found) for $C_{27}H_{44}BClN_7Rh$: C, 52.7 (51.0); H, 7.2 (7.1); N, 15.9 (14.4).

Preparation of Tp′Rh(Cl)(C_5H_9)(CNCH$_2$C(CH$_3$)$_3$) (3c). The synthesis of **3c** was identical to that of **3b** except that 70 mg (0.102 mmol) of **1** was dissolved in 5 mL of cyclopentane. Yield: 28 mg (46%) as a white solid. The product could be crystallized from a 1:1 hexane:THF solvent mixture at −20 °C. ^{1}H NMR (C_6D_6): δ 0.739 (s, 9 H, C(CH$_3$)$_3$), 1.748 (br s, 2 H, CH$_2$), 1.927 (br s, 2 H, CH$_2$), 2.097 (s, 3 H, pzCH$_3$), 2.163, (br s, 2 H, CH$_2$), 2.182 (s, 3 H, pzCH$_3$), 2.222 (s, 3 H, pzCH$_3$), 2.309 (s, 3 H, pzCH$_3$), 2.778 (s, 3 H, pzCH$_3$), 2.913 (s, 3 H, pzCH$_3$), 4.850 (br s, 1 H RhCH), 5.561, (s, 1 H, pzH), 5.628 (s, 1 H, pzH), 5.699 (s, 1 H, pzH). One CH$_2$ of the cyclopentyl and the NCH$_2$ of the neopentylisocyanide are presumed to be under the pzCH$_3$ resonances. ^{13}C{^{1}H} NMR (C_6D_6): δ 12.239, 12.873, 13.128, 14.392, 14.742, 15.379 (pzCH$_3$), 24.088, 25.100 (ringCH$_2$), 26.735 (C(*C*H$_3$)$_3$), 31.916 (*C*(CH$_3$)$_3$), 34.076 (ringCH$_2$), 34.235 (RhCH), 38.373 (ringCH$_2$), 56.347 (NCH$_2$), 106.621, 107.928, 108.935 (pzCH), 142.444, 142.674, 144.424, 150.918, 150.978, 153.197 (pzC$_q$). IR (KBr): 2528 (B–H), 2202 (CNR) cm^{-1}. Anal. Calcd (found) for $C_{26}H_{42}BN_7Rh$: C, 51.9 (52.7); H, 7.0 (7.2); N, 16.3 (15.5).

Preparation of Tp′Rh(Cl)(C_5H_{11})(CNCH$_2$C(CH$_3$)$_3$) (3d). The synthesis of **3d** was identical to that of **3b** except that 60 mg of **1** was dissolved in 3 mL of *n*-pentane. Yield: 38 mg (72%) as a white solid. The product could be crystallized from a 1:1 hexane:THF solvent mixture at −20 °C. ^{1}H NMR (C_6D_6): δ 0.722 (s, 9 H, C(CH$_3$)$_3$), 0.934 (t, J = 7.3 Hz, 3 H, alkylCH$_3$), 1.45 (complex mult, 2 H, CH$_2$), 1.72 (complex mult, 2 H, CH$_2$), 2.01 (complex mult, 2 H, CH$_2$), 2.088 (s, 3 H, pzCH$_3$), 2.151 (s, 3 H, pzCH$_3$), 2.227 (s, 3 H, pzCH$_3$), 2.382 (s, 3 H, pzCH$_3$), 2.648 (AB q 2 H, NCH$_2$), 2.787 (s, 3 H, pzCH$_3$), 2.985 (s, 3 H, pzCH$_3$), 3.30 (complex mult, 1 H, RhCH$_2$alkyl), 3.46 (complex mult, 1 H, RhCH$_2$alkyl), 5.566 (s, 1 H, pzH), 5.623 (s, 1 H, pzH), 5.708 (s, 1 H, pzH). ^{13}C{^{1}H} NMR (C_6D_6): δ 12.241, 12.726, 12.950, 14.561, 14.580, 14.603, 14.625 (pzCH$_3$ or alkylCH$_3$), 18.713 (d, J = 19 Hz, RhCH$_2$), 23.103 (alkylCH$_2$), 26.584 (C(*C*(CH$_3$)$_3$), 31.903 (*C*(CH$_3$)$_3$), 33.939 (alkylCH$_2$), 35.638 (alkylCH$_2$), 56.149 (NCH$_2$), 106.598, 107.675, 108.478 (pzCH), 142.484, 142.753, 144.288, 150.700, 151.079, 153.066 (pzC$_q$). IR (hexane): 2528 (B–H), 2199 (CNR) cm^{-1}. Anal. Calcd (found) for $C_{26}H_{44}BClN_7Rh$: C, 51.7 (51.6); H, 7.3 (7.5); N, 16.2 (16.2).

---

[22] Bryndza, H. E.; Fong, L. W.; Paciello, R. A.; Tam, W.; Bercaw, J. E. *J. Am. Chem. Soc.* **1987**, *109*, 1444. Schock, L. E.; Marks, T. J. *J. Am. Chem. Soc.* **1988**, *110*, 7701. Schaller, C. P.; Wolczanski, P. T. *Inorg. Chem.* In press.

[23] Elmitt, K.; Green, M. L. H.; Forder, R. A.; Jefferson, I.; Prout, K. *J. Chem. Soc., Chem. Commun.* **1974**, 747. Green, M. L. H.; Berry, M.; Couldwell, C.; Prout, K. *Nouv. J. Chem.* **1977**, *1*, 187. Berry, M.; Elmitt, K.; Green, M. L. H. *J. Chem. Soc., Dalton Trans.* **1979**, 1950. *J. Chem. Soc., Dalton Trans.* **1979**, 1979. Grebenik, P. D.; Green, M. L. H.; Izquierdo, A. *J. Chem. Soc., Chem. Commun.* **1981**, 186.

[24] Tsou, T.-T.; Loots, M.; Halpern, J. *J. Am. Chem. Soc.* **1982**, *104*, 623.

Table VIII. Summary of Crystallographic Data for Tp′Rh(Cl)(*n*-pentyl)(CN-neopentyl) (**3d**)

formula	$C_{26}H_{44}BClN_7Rh$
formula weight	568.40
crystal system	monoclinic
space group	$P2_1/c$
Z	4
a, Å	8.8865 (28)
b, Å	11.0816 (30)
c, Å	31.4597 (74)
β, deg	90.797 (22)
V, Å^3	3098 (2)
crystal dimensions, mm	0.11 × 0.19 × 0.34
T, °C	−75
radiation, Å (monochromator)	Mo, 0.710 89 (graphite)
2θ range, deg	2–44
no. of unique data $>3\sigma$	3214
no. of parameters varied	329
absorption coefficient, cm^{-1}	5.653
range of transmission factors	0.9256–1.0861
agreement between equivalent data	0.101
R_1/R_2	0.031/0.039
goodness of fit	1.622
largest peak in final E map	0.548

Preparation of Tp′Rh(Cl)($CH_2C_6H_3$-3,5-$(CH_3)_2$)($CNCH_2C(CH_3)_3$) (2f). The synthesis of **2f** was identical to that of **2b** except that 50 mg of **1** was dissolved in 3 mL of mesitylene. The crude product was purified by preparative thin-layer chromatography (5:1 THF:hexane on 1000-μm silica gel plate, 20 × 20 cm^2). Two products were isolated. The major product was **2f** (26 mg, 55%). A minor product (approximately 5 mg) is believed to be Tp′Rh$(Cl)_2$(CN-neopentyl) (7). For **2f**, ^1H NMR (C_6D_6): δ 0.555 (s, 9 H, $C(CH_3)_3$), 2.144 (s, 3 H, pzCH_3), 2.180 (s, 3 H, pzCH_3), 2.205 (s, 3 H, pzCH_3), 2.273 (br s, 9 H, overlapping pzCH_3 and arylCH_3), 2.782 (s, 3 H, pzCH_3), 3.039 (s, 3 H, pzCH_3), 4.118 (dd, J_1 = 9.8 Hz, J_2 = 2.7 Hz, 1 H, benzylH), 5.189 (dd, J_1 = 9.8 Hz, J_2 = 3.0 Hz, 1 H, benzylH), 5.538 (s, 1 H, pzH), 5.584 (s, 1 H, pzH), 5.677 (s, 1 H, pzH), 6.774 (s, 1 H, arylH), 7.606 (s, 2 H, arylH). $^{13}C\{^1H\}$ NMR (C_6D_6): δ 12.300, 12.647, 12.975, 14.783, 15.224, 16.760 (pzCH_3), 18.879 (d, J = 19.1 Hz, RhCH_2aryl), 21.555 (arylCH_3), 26.472 ($C(CH_3)_3$), 31.366 ($C(CH_3)_3$), 56.344 (NCH_2), 106.799, 107.676, 108.996 (pzCH), 125.906, 128.757, 136.365 (arylC), 137.74 (d, J = 55 Hz, RhCNR), 142.676, 142.737, 144.540 (pzC_q), 151.360 (arylC_q), 151.562, 153.146 (pzC_q). Anal. Calcd (found) for $C_{30}H_{44}BClN_7Rh$: C, 55.3 (54.7); H, 6.8 (6.7); N, 15.0 (14.3). For 7, ^1H NMR (C_6D_6): δ 0.790 (s, 9 H, $C(CH_3)_3$), 2.038 (s, 6 H, pzCH_3), 2.110 (s, 3 H, pzCH_3), 2.702 (s, 2 H, NCH_2), 2.730 (s, 6 H, pzCH_3), 3.230 (s, 3 H, pzCH_3), 5.495 (s, 2 H, pzH), 5.528 (s, 2 H, pzH). $^{13}C\{^1H\}$ NMR (C_6D_6): δ 12.150, 12.408, 15.384, 15.605 (pzCH_3), 26.511 ($C(CH_3)_3$), 32.296 (C-$(CH_3)_3$, 56.396 (NCH_2), 108.346, 108.847 (pzCH), 142.590, 144.218, 153.095, 155.367 (pzC_q).

Solution and Refinement of Crystal Structure for Tp′Rh(Cl)(*n*-pentyl)(CN-neopentyl) (3d). A well-formed crystal with approximate dimensions of 0.11 × 0.19 × 0.34 mm^3 was mounted on a glass fiber and placed on a Enraf–Nonius CAD4 diffractometer under a cold stream of nitrogen at −75 °C. The lattice constants were obtained from 25 centered reflections with values of χ between 10 and 60°. Cell reduction revealed a primitive monoclinic crystal system. Data were collected in accord with the parameters in Table VIII. The intensities of three representative reflections, which were measured after every 60 min of X-ray exposure time, remained constant throughout data collection, indicating crystal and electronic stability (no decay correction was applied). The space group was uniquely assigned as $P2_1/c$ on the basis of the systematic absences, and the correctness of this choice was confirmed by successful solution of the Patterson map, showing the rhodium atom. The structure was expanded by using the DIRDIF program supplied by the Molecular Structure Corp., whose programs were used for further refinement of the structure.[25] Anisotropic refinement of all non-hydrogen atoms allowed the use of a difference Fourier map for the location of the hydrogen atoms, the coordinates of which were subsequently idealized. An empirical absorption correction was applied by using the program DIFABS. Final anisotropic refinement was carried out on all non-hydrogen atoms with both the positional and thermal parameters "riding" on the atom to which they were attached.

Generation of Tp′Rh(CN-neopentyl)(CH_3)H. A solution of 10 mg (0.015 mmol) of **1** in cyclohexane was irradiated for 1 h in an ampule. The solution was then transferred to a high-pressure 30-mL bomb reactor and pressurized with methane (2300 psi). After the solution was allowed to stand for 18 h, the methane was vented and the solvent was removed under vacuum. The product was taken up in benzene and examined by ^1H NMR spectroscopy, showing **2k** as the major product. ^1H NMR (C_6D_6): δ −14.814 (d, J = 24.4 Hz, 1 H). Insufficient quantities were available from this method of preparation to permit full characterization.

Kinetics of Reductive Elimination Reactions of Compounds 2. An NMR sample containing 10 mg (0.015 mmol) of **1** and 0.5 mL of *n*-pentane was cooled in a 10 °C bath and irradiated ($\lambda > 340$ nm) until all of the solid had dissolved (~20 min). The solvent was removed under high vacuum, and C_6H_6 condensed into the tube. The tube was flame-sealed and placed in the probe of the NMR spectrometer (23 °C), and spectra were recorded every 2–5 min using a solvent suppression sequence. The hydride region of the spectrum showed the disappearance of **2d** and the appearance of **2a**. Integration of these resonances allowed for determination of the percent reaction, which was plotted as described in the text. Similar kinetic studies were made using cyclopentane, cyclohexane, and mesitylene. The rate of methane elimination was determined by preparing the sample as described above and dissolving in C_6H_6.

Sample Preparation and Photolysis Experiments for Determination of I_1/I_2. Runs 1–4. Solvent mixtures were prepared in accord with the ratios (V_1/V_2) shown in Table IV. To a 5-mm NMR tube containing a ground glass joint and vacuum line adapter under inert conditions was charged 10 mg (0.015 mmol) of **1** along with 0.14 mL of a deuterated solvent (runs 1 and 2, C_6D_6, runs 3 and 4, cyclohexane) and 0.45 mL of the solvent mixture. The sample was cooled to 78 K in liquid nitrogen, and the tube was flame sealed. The sample was warmed to 25 °C and then placed in the cooled NMR probe at −15 °C. After the sample was carefully shimmed, an initial ^1H NMR spectrum was acquired under standard conditions. The absolute frequencies of the solvent resonances were noted and entered into a frequency list, which was part of a multiple solvent peak suppression program. A second spectrum was obtained using the pulse program to ensure that the routine was properly suppressing the solvent resonances. The sample was placed into a cooled Pyrex dewar (ethanol/ice bath) at the temperatures shown for each experiment in Table IV. The sample was irradiated with high-intensity light (200 W Hg(Xe), $\lambda > 345$ nm) for the times indicated in Table IV. The sample was moved to the NMR spectrometer in the dewar. The sample was quickly placed into the cooled probe, and a ^1H NMR spectrum was taken immediately, the time for total acquisition being approximately 4 min. Subsequent NMR spectra were acquired at approximately 5-min intervals to ensure that there was no drastic change in the observed product ratios. **Run 5.** To a 5-mm NMR tube equipped as above was charged 5 mg of **1** and 0.42 mL of *n*-pentane. The solution was cooled to −78 °C, and the tube was evacuated on a high vacuum line. *n*-Propane was condensed into the tube. The tube was warmed to −40 to −50 °C, and the volume of the total solution was measured, from which the volume of propane was determined to be 0.35 mL (assuming no volume of mixing). The sample was irradiated as above at −40 to −50 °C for 5 min and then recooled to −78 °C. The propane was removed under vacuum, followed by removal of the pentane at 0 °C. The tube was cooled to −78 °C a third time, and cyclohexane-d_{12} was condensed in. The tube was flame sealed, and an NMR spectrum was acquired immediately in a preshimmed probe at −15 °C.

Acknowledgment is made to the U.S. Department of Energy (Grant DE-FG02-86ER13569) for their support of this work.

Supplementary Material Available: Tables of bond distances and angles, fractional atomic coordinates, and anisotropic thermal parameters (9 pages); tables of calculated and observed structure factors (20 pages). Ordering information is given on any current masthead page.

---

(25) $R_1 = (\Sigma||F_o| - |F_c||)/\Sigma|F_o|$, $R_2 = [\Sigma w(|F_o| - |F_c|)^2]^{1/2}/\Sigma wF_o^2$, where $w = [\sigma^2(F_o) + (\rho F_o^2)]^{1/2}$ for the non-Poisson contribution weighting scheme. The quantity minimized was $\Sigma w(|F_o| - |F_c|)^2$. Source of scattering factors f_o, f', f'': Cromer, D. T.; Waber, J. T. *International Tables for X-Ray Crystallography*; The Kynoch Press: Birmingham, England, 1974; Vol. IV, Tables 2.2B and 2.3.1.